

0346.4a

A-22

ОБЪЕДИНЕННЫЙ
ИНСТИТУТ
ЯДЕРНЫХ
ИССЛЕДОВАНИЙ
ДУБНА



19/8-74

E1 - 8047

3224/2-74

G.Adylov, F.Aliev, D.Bardin, W.Gajewski,
I.Ioan, B.Kulakov, G.Micelmacher, B.Niczyporuk,
T.Nigmanov, E.Tsyganov, M.Turala, A.Vodopianov,
K.Wala, E.Dally, D.Drickey, A.Liberman
P.Shepard, J.Tompkins, C.Buchanan, J.Poirier

THE PION RADIUS

1974

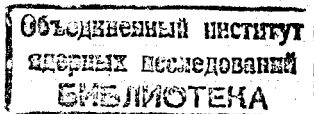
ЛАБОРАТОРИЯ ВЫСОКИХ ЭНЕРГИЙ

E1 - 8047.

G.Adylov, F.Aliev, D.Bardin, W.Gajewski,
I.Ioan, B.Kulakov, G.Micelmacher, B.Niczyporuk,
T.Nigmanov, E.Tsyganov, M.Turala, A.Vodopianov,
K.Wala, E.Dally,¹ D.Drickey,¹ A.Liberman¹
P.Shepard,¹ J.Tompkins,¹ C.Buchanan,¹ J.Poirier²

THE PION RADIUS

Submitted to XVII International Conference
on High Energy Physics, London, July 1-10,
1974.



¹ University of California, Los Angeles,
California.

² Notre Dame University.

I. INTRODUCTION

The pion electromagnetic radius has been directly measured by observing electrons scattered from 50 GeV/c pions taken from an internal target at the 76 GeV proton synchrotron at the Institute of High Energy Physics, Serpukhov. We find $\langle r_{\pi}^2 \rangle = (0.61 \pm 0.15)F^2$ from the analysis of the data comprising 40,000 events with recoiling electron energy between 13 GeV and 36 GeV. Because of the large statistical sample, the error is dominated by systematic effects.

The pion form-factor can be measured in both the space-like and time-like regions. In the space-like region, the only significant previous result from a direct measurement was by Cassels et al. ⁽¹⁾ who found $\langle r_{\pi}^2 \rangle^{1/2} < 3.3F$. The form factor has been indirectly measured at much larger space-like four-momentum transfers than available in the present experiment in inelastic electron-scattering experiments which isolate the one-pion exchange diagram. The most accurate result is by Brown et al. ⁽²⁾ who find $\langle r_{\pi}^2 \rangle^{1/2} = 0.70F$ with a very small statistical error. Time-like measurements have been made using e^+e^- colliding beams, ⁽³⁾ and connected to the space-like region via a dispersion relation. ^(4,5) These results can be summarized by the conclusion that the pion radius must be very near its ρ dominant value of 0.63F.

II. APPARATUS

Figure 1 shows the magnetostrictive-spark-chamber spectrometer used for the pion-electron scattering measurements. ⁽⁶⁾ Three blocks of spark chambers measured the direction of the incoming 50 GeV beam particle and

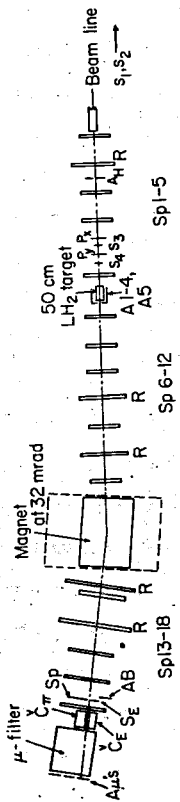


Fig. 1. The magnetostrictive-spark-chamber spectrometer used in the determination of the pion radius.

the momenta and scattering angles of the recoiling pion and electron.⁽⁷⁾ Chambers denoted by R were rotated 45° with respect to the rest of the block. Angles were typically measured to ± 0.15 mr, momenta to $\pm 0.4\%$. The beam momentum spread was either $\pm 2\%$ or $\pm 1\%$ depending on the momentum slit setting. The magnet field was calibrated to a precision of $\pm 0.2\%$.⁽⁸⁾ The second block of chambers (SP6-12) had readouts on each end of the magnetostrictive wand so that the narrow opening-angle pair could be accurately identified. Typical beam intensities were 2×10^5 particles per 1.2 second spill. The apparatus could accept up to 120 triggers every 6-second accelerator cycle. An important feature of the experiment was that the efficiency of only four counters (S_p , S_E , C_E , C_π) entered into the cross section. C_E and C_π were lead glass shower counters whose pulse height was measured on each event and whose efficiency could be measured off-line from these distributions.⁽⁹⁾ (We find both C_E and C_π to be 100.0 efficient within 0.1%) A large pulse height in one of these counters was required for a trigger; during a small part of the run this requirement was removed providing an additional check on these counters' efficiency and extending the accepted recoil electron energy below 17 GeV to 13 GeV for a sample of the data. The counters S_p and S_E placed in coincidence were thin scintillators each viewed by two phototubes, one on either side of the counter. The two signals, individually latched but in an electronic OR in the trigger provided a continuous monitor of the counters' efficiency; the inefficiency was found to be negligible. A muon filter consisting of 3m of iron provided some off-line information on muon contamination in the beam. Two sets of electronics were run in parallel in the experiment, and consistency to about the 1% level

was obtained. Anti-coincidence counters A1-4 around the target were latched but not used in the experiment. Counter A₅ (downstream from the target but with a hole such that few π -e events were rejected) and AB were placed in anti-coincidence. Their accidental rate was carefully monitored so that the appropriate correction to the cross section could be made. Additional corrections were made for unwanted anti-coincidences from delta rays accompanying a π -e event, and radiative gamma rays striking and converting in the counter. The 50 cm liquid hydrogen target was constructed so that the length and density could be accurately known. A special feature was the cylindrical copper shield inside the hydrogen which channeled bubbles away from the central region. The product of length times density for this target is known with an error $\pm 0.1\%$.⁽¹⁰⁾

III. DATA ANALYSIS

Approximately 2.5×10^6 triggers were taken in this experiment. The data were passed through a trackfinding program especially tailored to find pion-electron scattering events using the redundancy provided by many chambers. Although elastic scattering is, in principle, a four constraint process, only three of these are useful at high energy. The three constraints applied were longitudinal momentum balance, transverse momentum balance, and co-planarity. Each of these distributions separately shows a strong π -e signal, application of any one constraint identifies events with only a small background permitting each constraint to be applied by a relatively loose cut. Redundancy is further provided by a large pulse height for the electron in a shower counter. Pions and

electrons were identified by their scattering angles and the shower counter information. Two separate trackfinding programs, written at least partially independently, serve as one check that the fraction of π -e events found is known, although the π -e event finding efficiency for the programs differed. Many other checks were also made, and some of them are discussed below.

IV. CORRECTIONS

The determination of the absolute event-finding efficiency of the analysis programs is the most difficult correction. This correction was calculated by two separate, but apparently equivalent methods, each method used a Monte Carlo program based on the π -e events found in our data. In one, the real pion and electron sparks were removed from the event and sparks from a fake π -e event generated with the experimental errors were superimposed on the background sparks. These fake events were then analyzed by the trackfinding program to determine the event-finding efficiency. The model included statistical inefficiencies from chamber gaps and wand failures as well as losses from spark merging and wand deadtimes. As an example of the power of the method, comparison of the Monte Carlo and real data revealed an unexpected inefficiency for sparks located at separations less than 5mm in projection. This inefficiency was subsequently included in the analysis. In the second, fake events were analyzed by the trackfinding program to determine the trackfinding efficiency using Monte Carlo generated background tracks in the chambers. The gap and x- and y-wand efficiencies were found to be dependent on the number of background tracks in the spectrometer and

also on the distance between two tracks if it was less than 6mm. Beam intensity was reconstructed from appropriate counter data, and the beam profile was taken from special beam runs. Other parameters which influence the chamber efficiency to a lesser degree, such as the "age" of the background track, the number of events in the spill, etc., were taken into account very accurately by a phenomenological procedure so that the characteristics of the real and fake events should be in maximal agreement. The Monte-Carlo program also included the wand deadtime, experimental accuracies, multiple scattering, electron energy losses, and the operating conditions of the lead glass Čerenkov counters. Agreement of the relative efficiencies of different trackfinding programs for the real and fake data was a very rigid criterion for this calculation and gave confidence that all experimental effects had been taken into account.

These programs did not lead to completely consistent results disagreeing mainly on the absolute event-finding efficiency of the two final trackfinding programs. This disagreement, of about 2.5% for the more efficient program, contributes substantially to the overall systematic uncertainty in our result. Pi-e event-finding efficiencies for different data samples and for the two final programs used in our analysis varied from a low of 80% to a high of 98%, dependent upon experimental conditions for a particular sample and also upon the program used to estimate this efficiency.

Geometric efficiencies were also calculated by a Monte Carlo program. The geometric efficiency was dependent on the phase space of the incident beam, but these systematic effects were minimized

by using the appropriate average of experimentally measured beam distributions as input to the Monte Carlo. Positions and apertures in the spectrometer were carefully measured by surveying; the high statistics of this experiment permitted a close comparison of the data with many of these measurements to find, for example, counter edges. The Monte Carlo faithfully reproduces all of these distributions. Multiple scattering and bremsstrahlung were shown to have only a minor effect on the total geometric efficiency. Since the efficiency does vary with recoil electron energy, a valuable consistency check can be made by the fact that $|F_{\pi}|^2$ vs q^2 is nearly a straight line.

Radiative corrections have been calculated⁽¹¹⁾ taking full account of our experimental conditions and our cuts on the kinematic constraints. The results are sensitive to these experimental effects only at a level of ~1% since the cuts can be so loosely applied. The correction varies slightly from run to run in the experiment since it depends on the incoming beam momentum distribution which was used as input to the calculation. The geometric efficiency and the radiative correction as a function of recoil electron energy are shown in Figure 2. Bremsstrahlung in the target is not included as a part of this correction, but instead it is included in the calculation of the expected cross section.

All of the corrections to the data are shown in Tables I and II. Table I contains corrections which are q^2 dependent in principle. In practice, corrections 8 through 11 were treated as q^2 independent. The assigned errors are systematic. The corrections for geometrical efficiency, trackfinding efficiency, and the radiative correction also have statistical errors from the Monte Carlo calculation which varied

TABLE I: q^2 Dependent Corrections

Effect	Average Correction in %	Assigned Error
1. Geometric efficiency	See Fig. 2	$0.05(1-\epsilon)^*$
2. Event finding	variable, see text	$0.1 \delta^\dagger$
3. Radiative correction	See Fig. 2	0.05δ
4. Bremsstrahlung in target	10.0	0.05δ
5. Bremsstrahlung in spectrometer	9.0	0.05δ
6. π decay in flight	1.0	0.1%
7. Target empty I (measured)	3.9	0.4% (statistical)
8. Target empty II	1.0	0.1%
9. Background	0.0	0.5%
10. π attenuation in spectrometer	1.1	0.3%
11. π attenuation in hydrogen	5.0	0.2%
12. Target Z position cut losses	0.65	0.1%
13. μ -e scatters	0.7	0.2%
14. Spectrometer energy calibration	0.0	0.5%

* ϵ is the geometrical efficiency

† δ is the correction

TABLE II: q^2 Independent Corrections

Effect	Correction in %	
	I	II
1. Beam attenuation	2.1 ± 0.6	2.1 ± 0.6
2. $48 \text{ GeV} < E_{\text{Beam}} < 52 \text{ GeV}$	4.1 ± 0.2	5.1 ± 0.2
3. Accidental anti-coincidences	3.2 ± 0.7	2.2 ± 0.5
4. Beam scaler correction	1.0 ± 0.2	1.0 ± 0.1
5. K^-, \bar{p} beam contamination	1.2 ± 0.1	1.2 ± 0.1
6. μ^- (less than 50 GeV)	(included in 2 above)	
7. μ^- ($48 \text{ GeV} < E_{\mu} < 52 \text{ GeV}$) (correction to beam scalers)	0.52 ± 0.1	0.52 ± 0.1
8. Shower counter efficiency	0.0 ± 0.2	0.0 ± 0.2
9. Scintillator counter efficiency	0.0 ± 0.2	0.0 ± 0.2
10. Target delta rays in anti-coincidence	$1/25 \pm 0.25$	0.5 ± 0.25
11. Radiative photons in anti-coincidence	0.34 ± 0.2	0.80 ± 0.2
12. Liquid-hydrogen target thickness	0.0 ± 0.1	$0.0 \pm 0.2\%$

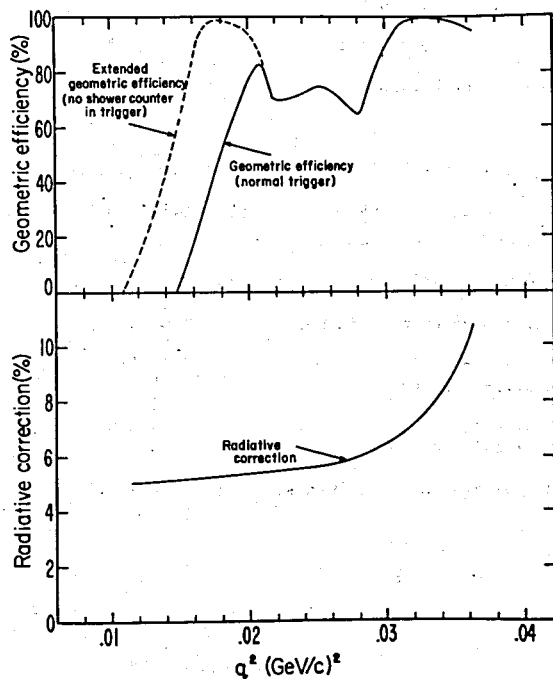


Fig. 2. a) A typical geometric efficiency vs. recoil electron energy as determined from a Monte Carlo calculation.
 b) The radiative correction for π -e scattering vs. recoil electron energy.

with q^2 . The systematic errors were treated as introducing a maximal positive correlation between all pairs of data points. The exceptions were the geometrical efficiency where only nearby data points were taken as correlated, and the spectrometer energy calibration where a sign change occurs in the correlation coefficient between some pairs of data points.

V. RESULTS

The square of the pion form factor as a function of q^2 is obtained by dividing the experimentally determined differential-cross sections after all corrections by the theoretical expected differential-cross sections for a point pion. These theoretical cross sections have been adjusted to compensate for realistic experimental conditions such as the incident momentum spectrum and real bremsstrahlung in the target and spectrometer. The resultant pion form factors squared as a function of q^2 are presented in Table III. The data are plotted with their total errors in Figure 3. Table III also contains the total errors in the data which include the effects of all systematic errors, and a matrix of correlation coefficients is given in Table IV.

The data were fitted to the form $|F_\pi|^2 = \frac{N}{(1 + Aq^2)^2}$ and the mean square pion radius was extracted using the fact that $F_\pi = 1 - 1/6 q^2 \langle r_\pi^2 \rangle + \dots$. The fit to the data employs the full error matrix including all systematic errors. The result is $\langle r_\pi^2 \rangle = (0.61 \pm 0.15)F_\pi^2$. The error is dominated completely by systematic effects, statistical errors contributing only $\pm 0.03F^2$. The effect of the systematic errors basically is to increase the overall normalization uncertainty of the

TABLE III: Experimental Results

Datum No.	$q^2(\text{GeV}/c)^2$	$ F_\pi ^2$	Statistical Error	Total Error
1	0.0138	1.002	0.059	0.079
2	0.0149	0.991	0.055	0.074
3	0.0159	0.986	0.053	0.069
4	0.0169	0.983	0.052	0.076
5	0.0179	0.990	0.057	0.077
6	0.0190	0.924	0.016	0.050
7	0.0200	0.916	0.015	0.048
8	0.0210	0.946	0.016	0.047
9	0.0220	0.948	0.019	0.050
10	0.0231	0.918	0.020	0.051
11	0.0241	0.896	0.023	0.052
12	0.0251	0.905	0.025	0.053
13	0.0261	0.896	0.028	0.055
14	0.0272	0.894	0.033	0.059
15	0.0282	0.912	0.034	0.060
16	0.0292	0.847	0.032	0.059
17	0.0302	0.873	0.038	0.062
18	0.0312	0.910	0.036	0.059
19	0.0323	0.856	0.043	0.067
20	0.0333	0.742	0.057	0.089
21	0.0343	0.886	0.059	0.081
22	0.0353	0.849	0.081	0.109

TABLE IV. Correlation Coefficients

Datum No.	1	2	3	4	5	6	7	8	9	10	11	12	13	14	15	16	17	18	19	20	21	
.26																						
.19	.21																					
.23	.25	.22																				
.18	.21	.20	.30																			
.22	.26	.27	.36	.36																		
.23	.25	.27	.30	.31	.46																	
.23	.25	.27	.26	.27	.42	.44																
.22	.24	.25	.23	.25	.41	.43	.43															
.22	.23	.25	.23	.23	.37	.40	.41	.44														
.21	.23	.24	.22	.22	.33	.37	.38	.40	.41													
.21	.22	.24	.22	.22	.33	.35	.36	.37	.38	.40												
.20	.21	.23	.21	.21	.21	.37	.33	.34	.34	.35	.36	.36										
.19	.20	.21	.19	.19	.19	.29	.31	.32	.30	.32	.32	.33	.34									
.19	.20	.21	.19	.19	.19	.29	.31	.31	.30	.29	.31	.32	.33	.33								
.19	.20	.22	.20	.20	.20	.30	.31	.32	.31	.30	.29	.30	.30	.30	.31							
.18	.19	.20	.19	.19	.19	.28	.30	.30	.29	.28	.28	.28	.27	.26	.26	.31						
.19	.20	.21	.20	.19	.30	.31	.32	.30	.30	.29	.28	.28	.27	.26	.26	.26	.26					
.16	.18	.19	.17	.17	.17	.26	.28	.28	.27	.27	.26	.26	.25	.23	.23	.23	.24	.24				
.12	.13	.14	.13	.13	.13	.20	.21	.21	.20	.20	.19	.19	.19	.18	.18	.18	.18	.19	.19			
.13	.14	.15	.14	.14	.14	.21	.22	.22	.22	.22	.21	.21	.21	.21	.21	.21	.21	.21	.21	.21	.21	.15
.09	.10	.11	.10	.10	.10	.15	.16	.16	.16	.16	.16	.16	.15	.15	.15	.15	.16	.16	.16	.16	.16	.17

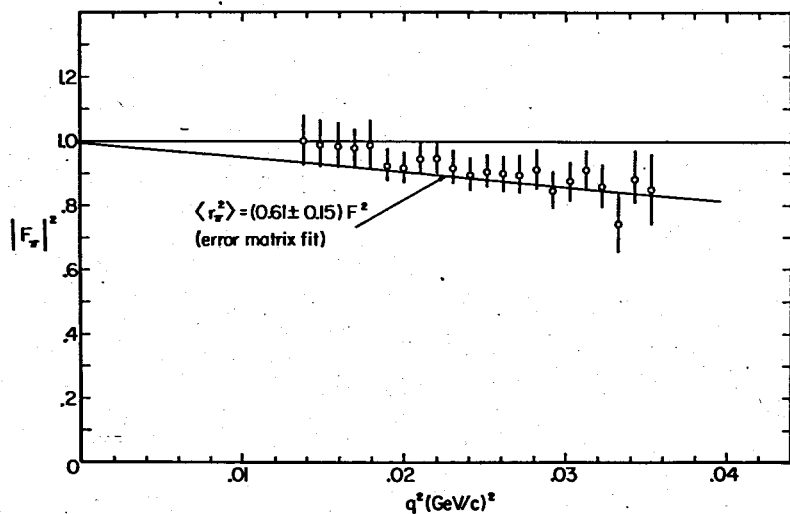


Fig. 3. $|F_\pi|^2$ vs. momentum transfer squared. The errors shown are the diagonal of the error matrix. Solid curves are shown for a point pion, and for the best fit to the data.

results. This systematic normalization error was estimated in Tables I and II to be approximately $\pm 2.8\%$.

We point out that two analyses of this data using somewhat different techniques do not arrive at completely consistent results. One program gives $\langle r_\pi^2 \rangle = 0.47 F^2$, the other gives $\langle r_\pi^2 \rangle = 0.72 F^2$. The form factors have been appropriately adjusted and the errors in the error matrix have been appropriately increased to take this effect into account. Various other checks of the data have been made, as one such check we fit the data to obtain $\langle r_\pi \rangle$ from the "slope" of the form factor alone. This method suspends the effects of systematic errors which primarily affect the overall normalization of data such as the trackfinding correction. This fit is accomplished by treating the normalization constant N as a free parameter and gives $\langle r_\pi^2 \rangle = (1.03 \pm 0.35) F^2$ and $N = 1.10 \pm 0.08$. An indication of the effects of systematic errors in the data can be obtained by comparing values of $\langle r_\pi^2 \rangle$ extracted using only the statistical errors. Requiring N to be 1.0 gives $\langle r_\pi^2 \rangle = (0.46 \pm 0.03) F^2$ allowing N to be a free parameter yields $\langle r_\pi^2 \rangle = (0.88 \pm 0.21) F^2$.

Our result represents the first direct measurement of the pion radius and can be compared both to the vector dominance prediction

$$\langle r_\pi^2 \rangle / \langle r_{\text{VDM}}^2 \rangle = 1.54 \pm 0.38$$

and to the size of the proton

$$\langle r_\pi^2 \rangle / \langle r_p^2 \rangle = 0.93 \pm 0.23$$

ACKNOWLEDGEMENTS

We express our thanks to the staff of IHEP for their aid in innumerable ways in the experiment. We especially thank Professor A. A. Logunov for his encouragement during the experiment as well as Professors Yu. D. Prokoshkin and R. M. Sulayev. Professor A. A. Naumov was of invaluable help in all matters related to accelerator operation. Dr. Yu. S. Khodirev worked closely with us during beam setup. Mr. J. Kieffer made significant contributions to the initial experimental setup. The American members of the group are especially grateful to Mr. V. I. Bodrov and his staff for their aid during their stay in Serpukhov. Professor A. M. Baldin and Professor H. K. Ticho supplied constant help and advice. We are grateful to Professor N. N. Bogolubov for his support and we also express our gratitude to Professor Glenn Seaborg, formerly Chairman of the U. S. Atomic Energy Commission and Professor A. M. Petrosyants, Chairman of the U.S.S.R. State Committee for the Utilization of Atomic Energy, without whose support and encouragement this experiment would not have taken place.

REFERENCES

1. David Cassel, "Experimental Measurement of the Electromagnetic Form Factor of the Negative π Meson". Ph.D. Thesis. Princeton University, 1964-65
2. C. N. Brown, et al., Phys. Rev. D, 9, 1229 (1974); and C. N. Brown, et al., to be published, London Conference Proc. 1974.
3. For example, see Orsay results: D. Benaksas, et al., Phys. Letters 39B, 289 (1972); Novosibirsk results: V. L. Auslander, et al., Soviet J. Nucl. Phys. 9, 69 (1969); and Frascati results: M. Bernardini, et al., Phys. Letters 46B, 261 (1973).
4. C. F. Cho and J. J. Sakurai, Lettere Nuovo Cimento 2, 7 (1971).
5. D. Levin and S. Okubo, Phys. Rev. D, 6, 3149 (1972).
6. G. T. Adylov, et al., "Experimental setup in a π -e scattering experiment at 50 GeV/c", JINR E13-6749 (1972).
7. G. T. Adylov, et al., "An on-line magnetostrictive spark chamber system used in a pion-electron scattering experiment at 50 GeV/c", JINR E13-6658 (1972).
8. W. Gajewski, et al., "Magnetic measurements for a π -e experiment at 50 GeV", JINR E13-6659 (1972).
9. G. Adylov, et al., "A Cerenkov total absorption shower counter", JINR E1-6976 (1973).
10. Yu. Borzunov, L. Golovanov, V. Mazarsky, A. Tsvinev, "The Precise Liquid Hydrogen Target", JINR P8-5212 (1970).
11. D. Yu. Bardin, G. V. Micelmacher, N. M. Shumaiko, "Calculation of the π -e Scattering Cross Section Involving the Radiative Correction and Realistic Experimental Condition." JINR E2-6235 (1972).

Received by Publishing Department
on June 26, 1974.